Contingent Pacific–Atlantic Ocean influence on multicentury wildfire synchrony over western North America

Thomas Kitzberger*†, Peter M. Brown‡, Emily K. Heyerdahl§, Thomas W. Swetnam¶, and Thomas T. Veblen‖

*Consejo Nacional de Investigaciones Científicas y Técnicas de Argentina and Laboratorio Ecotono, Universidad Nacional del Comahue, Quintral 1250, 8400 Bariloche, Argentina; ‡Rocky Mountain Tree-Ring Research, Inc. , 2901 Moore Lane, Ft. Collins, CO 80526; §U.S. Department of Agriculture Forest Service, Rocky Mountain Research Station, 5775 U.S. West Highway 10, Missoula, MT 59808; ¶Laboratory of Tree-Ring Research, University of Arizona, Tucson, AZ 85721; and ‖Department of Geography, University of Colorado, Boulder, CO 80301

Edited by Christopher B. Field, Carnegie Institution of Washington, Stanford, CA, and approved November 8, 2006 (received for review July 19, 2006)

Widespread synchronous wildfires driven by climatic variation, such as those that swept western North America during 1996, 2000, and 2002, can result in major environmental and societal impacts. Understanding relationships between continental-scale patterns of drought and modes of sea surface temperatures (SSTs) such as El Niño-Southern Oscillation (ENSO), Pacific Decadal Oscillation (PDO), and Atlantic Multidecadal Oscillation (AMO) may explain how interannual to multidecadal variability in SSTs drives fire at continental scales. We used local wildfire chronologies reconstructed from fire scars on tree rings across western North America and independent reconstructions of SST developed from tree-ring widths at other sites to examine the relationships of multicentury patterns of climate and fire synchrony. From 33,039 annually resolved fire-scar dates at 238 sites (the largest paleofire record yet assembled), we examined forest fires at regional and subcontinental scales. Since 1550 CE, drought and forest fires covaried across the West, but in a manner contingent on SST modes. During certain phases of ENSO and PDO, fire was synchronous within broad subregions and sometimes asynchronous among those regions. In contrast, fires were most commonly synchronous across the West during warm phases of the AMO. ENSO and PDO were the main drivers of high-frequency variation in fire (interannual to decadal), whereas the AMO conditionally changed the strength and spatial influence of ENSO and PDO on wildfire occurrence at multidecadal scales. A current warming trend in AMO suggests that we may expect an increase in widespread, synchronous fires across the western U.S. in coming decades.

Atlantic Multidecadal Oscillation | El Niño Southern Oscillation | fire history network | ocean warming | Pacific Decadal Oscillation

Wildfires are clearly driven by interannual variation in weather, but our understanding of the effects of multiannual to multidecadal spatial variations in fire-climate patterns in western North America and their relationship to broader-scale ocean–atmosphere patterns is incomplete. Linkages between fire and climate at broad spatial scales are evident when many large fires occur synchronously across broad regions during severe and extensive droughts lasting multiple seasons, such as the recent dry spell from 1999 to 2004. Recent advances in our understanding of ocean–atmosphere patterns and their influences on climate in western North America suggest that contingent states of sea surface temperature (SST) and atmospheric pressure in both the Pacific and Atlantic Basins may synchronize drought and hence fires in the western U.S. Moreover, climate and fire in different regions (e.g., the Pacific Northwest versus the Southwest), may respond in unique ways to these ocean–atmosphere conditions and their associated circulation patterns.

Both Pacific and Atlantic conditions appear to be involved in climate teleconnections in western North America, although precise mechanisms are only beginning to be understood (1–6). Observational and modeling studies (using global circulation models) consistently show that Pacific SSTs play an important role in driving interannual to decadal moisture and temperature patterns in this region (3, 4, 6). Dry or wet episodes are relatively stronger or weaker in particular times and regions, depending on the contingent state of El Niño Southern Oscillation (ENSO; seasonal to interannual variations in SSTs in the tropical Pacific), and Pacific Decadal Oscillation (PDO) (variations in SSTs in the north Pacific with a typical cycle of ≈20 years) (7, 8). Accumulating evidence from observations and modeling indicates that the Atlantic Multidecadal Oscillation (AMO; variations in SSTs in the north Atlantic that tend to adopt warm or cool modes at a ≈60-year cycle) is probably also involved in North American climate patterns (1–6, 8). Contingent SST conditions in both the Pacific and Atlantic seem to be particularly important, such as the coincidence of positive phases of the PDO and AMO, that resulted in drier conditions that persisted for a decade or longer in the northern tier of western U.S. states, extending into the Great Plains, during the 1930s drought (1, 2, 5, 7). In contrast, the coincidence of positive AMO and negative PDO phases were typically associated with dry and hot conditions across the southern tier of western states, as occurred during the 1950s drought. Likewise, La Niña events (occurring at scales of seasons to years) were typically related to the strongest droughts in the Southwest during the negative phase of the PDO (occurring at scales of years to decades) (7). In some combinations, these ocean–atmosphere oscillations produce particularly strong and spatially coherent dipole patterns of opposite dry/wet conditions in the Pacific Northwest versus the Southwest (2, 7, 9, 10).

Links between contingencies of ENSO and PDO, droughts and wildfires have been noted in the western U.S. before, but only for subregions (11–13) or using 20th century data (10, 14). Furthermore, AMO–fire teleconnections and contingencies with ENSO and PDO previously have been shown for single study areas but have not been examined at regional scales (15, 16). The recent availability of multicentury tree-ring width reconstructions of ENSO (Niño-3 Pacific SST 5°N-5°S, 90–150°W) (17), PDO (standardized leading PC of monthly SST anomalies in the North Pacific poleward of 20°) (18), and AMO (10-year running mean of detrended SST anomalies averaged over the North Atlantic Basin

Author contributions: T.K., P.M.B., E.K.H., T.W.S., and T.T.V. designed research; T.K. performed research; T.K., P.M.B., E.K.H., T.W.S., and T.T.V. analyzed data; and T.K., P.M.B., E.K.H., T.W.S., and T.T.V. wrote the paper.

The authors declare no conflict of interest.

This article is a PNAS direct submission.

Abbreviations: SST, sea surface temperature; ENSO, El Niño Southern Oscillation; PDO, Pacific Decadal Oscillation; PC, principal component; PDSI, Palmer Drought Severity Index; AMO, Atlantic Multidecadal Oscillation.

†To whom correspondence should be addressed. E-mail: kitzberger@gmail.com.

This article contains supporting information online at www.pnas.org/cgi/content/full/0606078104/DC1.

Table 1. Description of the North American tree-ring-based fire history database used in this study obtained from the International Multiproxy Paleofire Database, World Data Center for Paleoclimatology (www.ncdc.noaa.gov/paleo/impd/paleofire.html)

Region	Location	Number of sites	Number of fires (scars)	Number of fires (scars) by 1550 CE	Number of fires (scars) by 1700 CE
SMO	Sierra Madre Occidental, Mexico	8	231 (1,469)	0 (0)	2 (2)
AZ	Arizona	20	276 (4,785)	3 (21)	63 (605)
SNM	Southern New Mexico	37	430 (3,791)	4 (51)	58 (558)
NNM	Northern New Mexico	41	462 (6,013)	25 (120)	150 (1,147)
SCO	Southern Colorado	29	243 (2,109)	19 (105)	82 (512)
NCO	Northern Colorado	14	102 (1,155)	2 (11)	23 (129)
BHI	Black Hills, South Dakota	29	320 (1,980)	5 (26)	90 (435)
SNE	Sierra Nevada, California	54	1,220 (6,091)	26 (181)	188 (1,024)
PNW	Blue Mountains, Oregon, Washington Southern British Columbia, Canada	6	229 (5,646)	5 (25)	61 (627)
Total		238	3,513 (33,039)	89 (540)	717 (5,039)

from 0 to 70° N) (19), and independent networks of fire-scar chronologies enables us to evaluate continental-scale fire climatology over multiple centuries.

Results and Discussion

Our data set included a total of 33,039 annually resolved fire-scar dates from >4,700 fire-scarred trees in nine regions in western North America (Table 1).

Almost half the variance in fire occurrence among the nine subregions was explained by the first two components from a rotated principal components (PCs) analysis of the annual percentage of sites recording fire (%SF; 1550–1924; PC1 and PC2, 31% and 15%, respectively). Fires were highly synchronous within the Southwest (AZ, SNM, NNM, and SCO, see Table 1) but usually asynchronous between the Southwest and the Pacific Northwest (Fig. 1).

Correlations of these components with summer Palmer Drought Severity Index (PDSI) (Fig. 2 *A* and *B*) revealed broad northern and southern areas of common variation. In general, it appears that PC1 captured variations at interannual time scales, likely reflecting the influence of ENSO on fire across western North America, whereas PC2 captured variation at decadal scales, likely reflecting the influence of PDO in the Pacific Northwest.

Significant correlations of the first component, PC1, and PDSI were negative in the Southwest, indicating drought ($r < -0.3$, $P < 0.0001$), but positive in the Pacific Northwest and southwestern Canada ($r > 0.1$, $P < 0.05$). This finding resembles the typical dipole pattern of precipitation and drought related to ENSO interannual variability (2, 7), (Fig. 2*A*), and, indeed, this component was most strongly correlated with NINO3 (Fig. 2*C*; $r = -0.48$, $P < 0.0001$). Although these two patterns, PC1 and PC2, account for much of the variation in fire years, fire synchrony in some years differed from these two patterns. For example, when we forced the 238 binary fire chronologies into five clusters, fires were synchronous in the Sierra Nevada, Arizona, and New Mexico or over the entire western U.S. [supporting information (SI) Fig. 6]. Wavelet spectra of the PC1 scores showed a significant global maximum at a 4- to 5-year periodicity ($P < 0.05$, compared with red noise spectrum, SI Fig. 7), similar to ENSO periodicity.

In the Southwest, northwestern Mexico, and the south-central Rocky Mountains, production of the fine fuels that carry forest

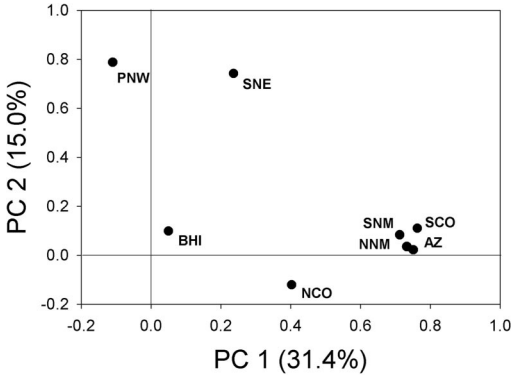

Fig. 1. Loadings of the first two PCs of a rotated principal components analysis of percentage of sites with fire scars (%SF) plotted in PC1–2 space.

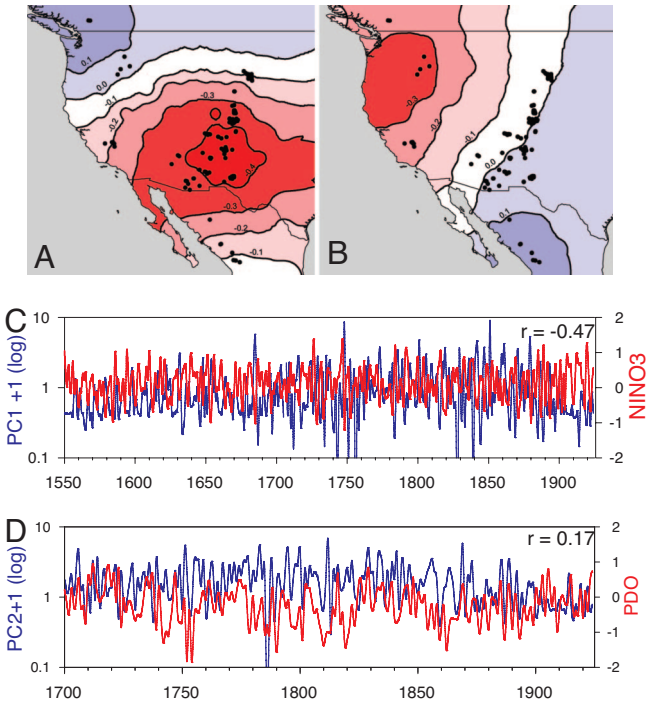

Fig. 2. Spatial and temporal patterns of fire correlations with PDSI and SST indices. (*A* and *B*) Correlations between the scores of the first two components of a rotated principal components analysis (PCA) of percentage sites with fire scars (%SF) and gridded tree-ring reconstructed PDSI in the conterminous U.S. for the period 1550–1925. Scores from the first two components of a varimax rotated PCA of the %SF (log scale, blue). (*C* and *D*) Superimposed on PC1 and PC2 scores are reconstructed NINO3 and reconstructed PDO (red line).

Table 2. Three-way combinations of contingent states

	SMO	AZ	SNM	NNM	SCO	NCO	BHI	SNE	PNW
SMO	**A+P-N-**	**A+P-N-**	**A+P-N-**	**A+P-N-**	*A+P-N-*	**A+P-N-**	**A+P-N-**	**A+P-N-**	**A+P-N-**
					A-P-N-				
AZ			A+P-N-	A-P-N-	A+P-N-	**A+P-N-**	A+P-N-	A+P-N-	A+P-N-
					A-P-N-		A-P+N+	*A-P+N+*	*A-P+N+*
SNM			**A+P-N-**	**A-P-N-**	*A+P-N-*	**A+P-N-**	*A+P-N-*	*A+P-N-*	*A+P-N-*
			A-P-N-		*A-P-N-*		A-P+N+		*A-P+N-*
NNM				**A-P-N-**	**A-P-N-**	**A+P-N-**	*A+P-N-*	*A-P-N-*	A+P-N-
					A+P-N-				*A-P+N-*
SCO					**A-P-N-**	**A+P-N-**	**A+P-N-**	*A+P-N-*	*A-P+N-*
								A-P-N-	
NCO						**A+P-N-**	**A+P-N-**	**A+P-N-**	**A+P-N-**
BHI							**A+P-N-**	**A+P-N-**	A+P-N-
SNE								*A-P+N+*	*A-P+N+*
PNW									**A-P+N+**

Three-way combinations of contingent states of ENSO (E), PDO (P), and AMO (A) during which observed fires were synchronous within regions (years with >5% of sites with synchronous fires, shown in diagonal cells that are enclosed in black lines) or between regions (fire years recorded at ≥1 site in each region, nondiagonal cells) above that expected by chance (bold, $P < 0.01$; italics, $P < 0.05$; normal, $P < 0.10$, χ^2 tests); +, warm phase; −, cold phase. All phase combinations occurred during the period analyzed (1700–1900). Phase combinations during which fire synchrony was not significantly above that expected by chance are not shown. The four significant phase combinations are color coded (gold, warm AMO, cold PDO, La Niña; blue, cold AMO, cold PDO, La Niña; green, cold AMO, warm PDO, El Niño; purple, cold AMO, warm PDO, La Niña).

fires, such as grass and needle litter, is increased during wet years, which are often associated with warm ENSO events (20). When these warm events are followed by La Niña events, with their associated dry conditions, fires are synchronized across this region (21, 22).

Lagged correlations between PC1 and PDSI (SI Fig. 8) confirm the importance of prior wet years in synchronizing fire across the Southwest (10, 20, 21). PC1 was correlated with −2 year-lagged PDSI in the Southwest (AZ, SNM, NNM, NCO, SMO ; $r > 0.1$–0.2, $P < 0.001$) and with −1 year-lagged PDSI in these regions plus Colorado and northern Mexico ($r > 0.1$, $P < 0.05$).

In contrast to the influence of ENSO in the Southwest, warmer/drier conditions in the Pacific Northwest are associated with El Niño events, typically resulting in earlier melting of snowpack, and hence a longer fire season, leading to synchronous fires in this subregion (23, 24). Lagged correlations between PC1 and PDSI were not significant in the Pacific Northwest, where fine fuel amount apparently does not limit forest fire occurrence at these temporal and spatial scales.

Significant correlations of the second component, PC2, with PDSI were negative in the Pacific Northwest, southwestern Canada, and northern California ($r < -0.3$, $P < 0.0001$; Fig. 2*B*) and weakly positive in northern Mexico ($r > 0.1$, $P < 0.05$). This component was correlated with PDO ($r = 0.17$, $P < 0.05$, 1700–1899; Fig. 2*D*). Furthermore, wavelet spectra of the PC2 scores show a nonsignificant peak at ≈10- to 20-year period (SI Fig. 7), similar to that for PDO. PC2 was not significantly correlated with lagged PDSI (SI Fig. 8).

In contrast to the influence of ENSO and PDO on fire synchrony, which varies among regions, positive AMO appears to synchronize fire across western North America at multidecadal time scales. Warm AMO phases were related to higher-than-expected fire synchrony in 32 of 36 possible interregional comparisons (89%) comprising most regions of western North America (Table 2). Cool AMO produced a lower degree of synchrony (50%) over relatively smaller regions such as the Southwest (with negative PDO and La Niña conditions) and the Pacific Coast (with positive PDO and El Niño conditions; Table 2).

The degree of synchrony in fire between all pairs of regions, varied during the past 475 years, consistent with variation in AMO (19) (Fig. 3 and SI Tables 3 and 4). A smoothed time series of AMO (10-year spline) was moderately correlated with multidecadal fire synchrony variation at the continental scale ($r = 0.50$ and 0.43, for the synchrony and dipole indices, respectively; $P < 0.001$; 1550–1924; Fig. 3). In contrast, multidecadal fire synchrony variation was not significantly correlated with annual and 50-year smoothed PDO or NINO3.

AMO and multidecadal fire synchrony show similar subcontinental spatial patterns when correlated with low-frequency variations in reconstructed PDSI (Fig. 4). Multidecadal periods of synchronous fire and drought spatially mirror the broad-scale pattern of multidecadal correlation of drought with AMO (2). Drought and warm AMO are correlated from northern Mexico to the U.S. Rocky Mountains–Great Plains and in the Pacific Northwest and southwestern Canada. In contrast, southern California to south-central Canada had above average moisture during these multidecadal periods of warm AMO and synchronous fire (Fig. 4).

The association of AMO and continental-scale synchrony of fire across western North America is consistent with the role of AMO in determining patterns of drought across the western U.S. (1, 2, 5). Fire was strongly synchronous across western North America during 1650–1770 (except 1710–1725) and after 1880

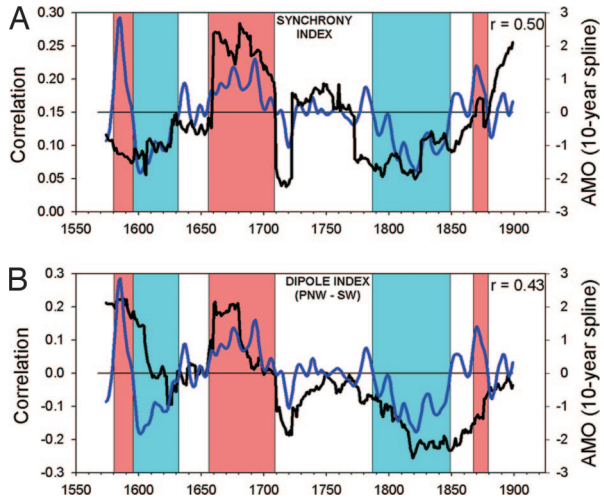

Fig. 3. Indices of fire synchrony (50-year moving correlations between selected regions, black line) compared with a 10-year spline of reconstructed AMO (blue line). Light blue and light red shaded areas indicate periods of low and high AMO, respectively, as defined by intervention analysis (19). Synchrony index was computed as the mean of all pairwise 50-year running correlations of %SF for all region pairs and reflects overall fire synchrony. Dipole Index was computed as the mean of all pairwise 50-year running correlations between the %SF of the Pacific Northwest and combined Southwest regions (AZ, SNM, NNM, and SCO) and reflects the degree of synchrony or asynchrony along the north–south dipole.

and weakly synchronous during 1550–1649 and 1750–1849 (Fig. 3*A*). The highest degree of fire synchrony occurred from 1660 to 1710, coincident with the longest and warmest phase of the AMO during the past five centuries (19). Conversely, the lowest degree of fire synchrony occurred from 1787 to 1849, coincident with the coldest phase of the AMO (19). This period is also unique in that it includes multiple decades of reduced fire occurrence in many areas of the western U.S. (15, 16, 22, 23, 25), and perhaps a shift in the seasonal timing of fires as well (26). A similar gap occurs in fire occurrence in northern Patagonia, Argentina (25), and may be associated with a reduced amplitude and frequency of ENSO events. The period 1810–1830 is also a particularly cold period in the northern hemisphere (27), and coincides with major volcanic eruptions. Therefore, multiple climatic causes for this intercontinental gap in fire occurrence are possible.

Our spatiotemporal analyses generally support other studies that show the varying regional importance of ENSO and PDO to climate in western North America, but in the context of fire occurrence and synchrony. Synoptic mechanisms for most of these teleconnections are fairly well understood, such as the effect of ENSO on the strength and position of northern and southern jet streams and the resulting north–south dipole pattern of precipitation (28). During the positive phase of the PDO, quasistationary blocking ridges of high pressure reduce precipitation over the Pacific Northwest by diverting storm tracks, leading to regional drying of fine fuels and synchronous fires across the region (24, 29). Our results are also consistent with changes in the relative importance of PDO to drought contingent on the phase of AMO over the past 500 years in the western U.S (2). We performed rotated PC analysis of %SF by region during warm, cold, and neutral states of AMO as defined by intervention analysis (19). The results (Fig. 5) show that the Pacific Northwest and Southwest are consistently opposite in their drought-fire phases.

However, when AMO is positive, fire tends to be synchronous over a large region from the Southwest to the Black Hills in the northern Rockies (Fig. 5), whereas drought tends to extend from the Southwest to the Northern Rockies and upper Colorado River basin (Fig. 4). During negative AMO, there is a reduced core of synchronous fire in the Southwest. During neutral AMO periods, a stronger north–south pattern emerges with synchrony between the Pacific Northwest and the Black Hills and a weak tendency for synchronous fire in the Sierras and Northern Colorado. These patterns are consistent with the interpretation based on hydrologic reconstructions that, during neutral phases of AMO, PDO becomes more dominant (2) through teleconnections with winter precipitation (30).

Mechanisms for AMO influence on western U.S. precipitation are the least well understood of the modes of SST variability that we examine here, and it is possible that the teleconnections we identified are spurious or aliasing other relationships. However, recent modeling supports the idea that North Atlantic SSTs are involved in North American climate patterns, potentially operating via a complex set of interactions and the effects of Rossby waves, thermohaline circulation, and wind patterns in the western Pacific (5, 6). Whatever the actual mechanisms of North Atlantic influence may be, our results with spatially and temporally extensive and independent fire-scar data indicate that, in addition to Pacific Ocean influences (ENSO and PDO), the extent of regional synchrony in reconstructed fire occurrence for western North America is statistically associated with at least one proxy reconstruction of North Atlantic SST variability (19).

Our network of accurately dated fire scars demonstrates the potential of broad networks of tree-ring reconstructions for evaluating long-term spatial and temporal climate-fire patterns across western North America. Our network suffers from limitations common to proxy data sets (e.g., decreasing sample size, and therefore increasing uncertainty with increasing time before the present). However, recent analyses of the modern climate forcing of area burned show that proxy time series can faithfully preserve climate–fire relationships (10) that persist into the

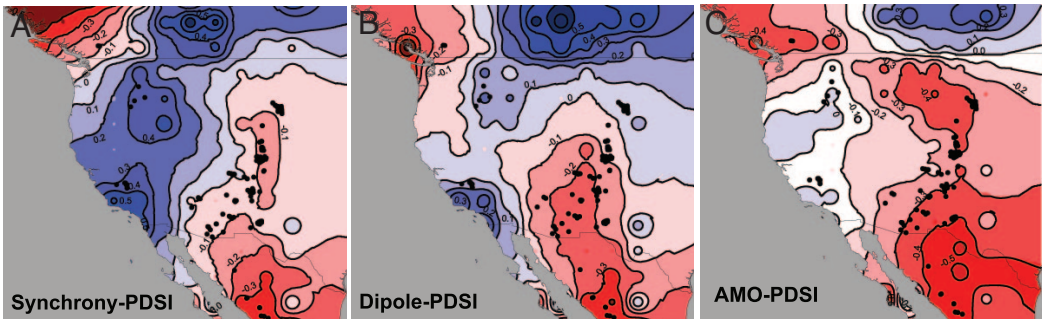

Fig. 4. Correlations between the fire synchrony index (*A*), the dipole fire index (*B*), and the 49-year running mean AMO (*C*) with a time-smoothed version (49-running mean) of gridded tree-ring reconstructed PDSI for the period 1574–1899.

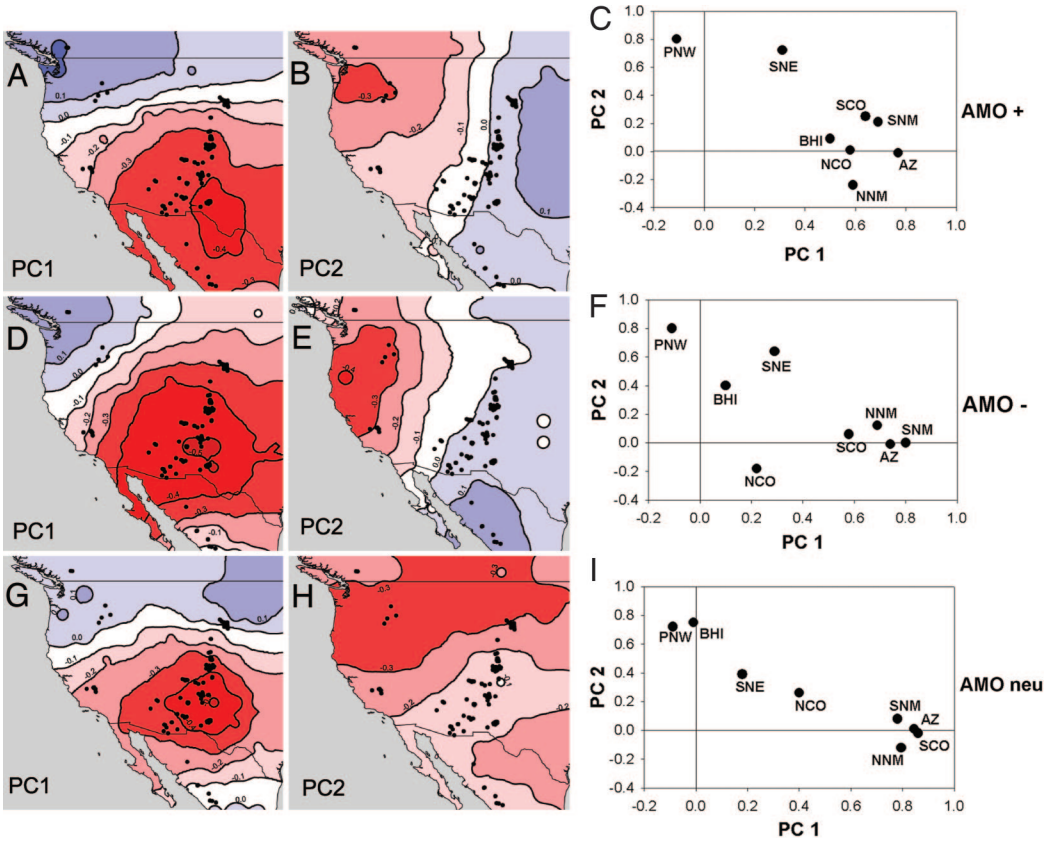

Fig. 5. Rotated principal components analysis of percentage of sites with fire scars (%SF) by region performed separately for AMO-positive (*A–C*), AMO-negative (*D–F*), and AMO-neutral periods (*G–I*) as defined by intervention analysis (19). (*A*, *B*, *D*, *E*, *G*, and *H*) Correlations between the scores of the first two components of a rotated principal components analysis and tree-ring reconstructed PDSI grid. (*C*, *F*, and *I*) Loadings of the first two principal components of the rotated principal components analysis of %SF.

modern period of fire records based on observations and instrumental data sets (14). Based on our current analyses, we suggest that both ENSO and decadal-scale states of the major ocean basins (Pacific and Atlantic) can be useful guides to potential forest fire hazards. Variation in ENSO appears to be the main driver of within-region synchrony at a quasi-annual scale, but at a multidecadal scale, AMO drives broad patterns in wildfire synchrony.

The current state of the AMO, which is trending positive (www.cdc.noaa.gov/Pressure/Timeseries/AMO), may presage increased fire synchrony in the western U.S. in the near future. Probabilities of future climatic regime shifts have been calculated using probabilistic projections based on the tree-ring reconstruction of AMO (31). However, prediction of risk of future climate shifts based on probabilistic projections from past climate variability is seriously complicated if global warming is a major driver of temperature trends in the North Atlantic (32). Moreover, recent analysis of fire and hydroclimatic data from western U.S. forests indicates that warming temperatures and earlier springs may already be driving increased occurrence of large wildfires, and longer fire seasons in the past two decades (33). As others have noted (5) these two influences (global or regional warming trends and positive AMO) may not add linearly, but either separately or combined these broad-scale climate trends do not bode well for ecosystems and human communities at risk from increasing wildfire hazards in the western U.S.

Materials and Methods

Individual fire chronologies comprising the network were based on an average of 20 fire-scarred trees in each of 238 sample sites that typically ranged in size from 10 to 100 ha and were obtained from the International Multiproxy Paleofire Database, World Data Center (WDC) for Paleoclimatology (www.ncdc.noaa.gov/paleo/impd/paleofire.html) and other collections held by the authors. Multiple fire scars are created when a tree survives repeated wounding by frequent, low-severity fires during which the vascular cambium is lethally heated around a portion of the circumference of the lower bole. The exact calendar year of fire occurrence is obtained by noting the year of the tree ring in which these scars occur. For each site, we constructed binary fire chronologies ("0" for nonfire, "1" for fire years) for two periods (1550–1924 and 1700–1924) of contrasting length and sample depth (Table 1). We defined fire years as those during which ≥10% of trees (and a minimum of two trees) had a fire scar. To identify the main patterns of fire synchrony among sites, we performed cluster and PC analyses. K-means clustering of the 238 binary fire chronologies was performed by forcing identification of the five clusters with greatest possible dissimilarity in fire synchrony based on the Ochiai index (1700–1899). Varimax rotated principal component analyses were run for the nine regions based on the annual percentage of sites recording fire (%SF; 1550–1924). We correlated cluster means or scores of the first components of a rotated principal components analysis of %SF with 0 year, -1 year, and -2 year lagged PDSI reconstructed from tree rings and gridded for the conterminous United States for the period 1550–1925 (34). The climate indices we used were reconstructed from tree-ring widths, which can vary in response to limiting climate factors. Trees sampled for fire scars were not used in the construction of climatic indices, and, indeed most trees used in the paleoclimatic indices were located at considerable distance from sites sampled for fire history. Thus, the

samples for developing past fire and past climate were independently derived. PDSI was obtained from the WDC for Paleoclimatology, National Oceanographic and Aeronautic Administration/National Geophysical Data Center (NOAA/NGDC), Boulder, CO (www.ncdc.noaa.gov/paleo/pdsidata.html). Scores of the two first principal components were correlated with tree-ring reconstructions of ENSO, PDO, and AMO obtained at the WDC for Paleoclimatology, NOAA/NGDC (ftp://ftp.ncdc.noaa.gov/pub/data/paleo/treering/reconstructions/nino3_recon.txt, ftp://ftp.ncdc.noaa.gov/pub/data/paleo/treering/reconstructions/pdo-darrigo2001.txt, and ftp://ftp.ncdc.noaa.gov/pub/data/paleo/treering/reconstructions/amo-gray2004.txt, respectively). The index of ENSO we used was reconstructed from earlywood and total tree-ring widths at 23 sites in the southwestern U.S. and Mexico (17). The index of PDO was reconstructed from tree-ring density and ring-width chronologies from nine sites in the U.S. and two sites in Mexico (19). The index of AMO was reconstructed from 12 tree-ring width chronologies from sites in Finland, France, Italy, Jordan, Norway, Russia, Turkey, and the U.S. (19). Spectral properties were explored with wavelet power spectra using the Morlet wavelet (35). Significance regions of the power spectrum were determined by using a red-noise (autoregressive lag1) background spectrum and cone of influence region was delimited where zero padding had reduced the variance.

We developed several indices of fire synchrony and asynchrony across the network to compare to climate indices. A fire synchrony index was computed as the mean of all pairwise 50-year running correlations for all regions and reflects overall fire synchrony. A dipole index was computed as the mean of all pairwise 50-year running correlations between the Pacific Northwest and combined Southwest regions (AZ, SNM, NNM, amd SCO; see Table 1) and reflects the degree of synchrony or asynchrony along a north–south axis.

We correlated the two indices of fire synchrony with reconstructed AMO (smoothed with a 10-year spline). Because of high autocorrelations inherent in moving correlations between time series, we used a Monte Carlo procedure to develop confidence intervals against which actual correlation coefficients were compared. Time series of %SF were shuffled 1,000 times within each region to derive confidence intervals. In each replicate, 50-year moving correlations between pairs of regions, the fire-synchrony index, and correlations with reconstructed AMO were calculated. The resulting 95th and 99th percentiles of the resulting correlations were then compared with the observed correlation between the fire synchrony index and reconstructed AMO. Fire synchrony indices were also correlated with time-smoothed (49-year running mean) reconstructed PDSI and compared with the correlation structure generated by smoothed (49-year running mean) reconstructed AMO.

We assessed fire synchrony (period 1700–1899) based on two procedures: (*i*) identification of years with >5% SF, and (*ii*) a χ^2 statistical comparison of observed and expected numbers of synchronous fire years (defined as more than one site in each region recording fire in that year) during years of the eight different possible combinations of positive and negative phases of climate drivers (AMO, PDO, and ENSO).

We thank T. Schoennagel and two anonymous reviewers for commenting on the manuscript, J. Betancourt for helpful discussions and comments on the manuscript, and the numerous students and colleagues who helped develop the fire-scar chonologies. This work was funded by Fundación Antorchas (T.K.), Consejo Nacional de Investigaciones Científicas y Técnicas de Argentina (T.K.), U.S. Department of Agriculture Forest Service–Rocky Mountain Research Station (P.M.B., E.K.H., and T.W.S.), U.S. Geological Service Biological Resources Division (T.T.V. and T.W.S.), U.S. Department of Interior, National Park Service (P.M.B. and T.W.S.), The Nature Conservancy (T.W.S.), City of Boulder Open Space Department (T.T.V.), and National Science Foundation Award DEB-0314305 (to T.T.V.).

1. McCabe GJ, Palecki MA, Betancourt JL (2004) *Proc Natl Acad Sci U.S.A* 101:4136–4141.
2. Hidalgo HG (2004) *Water Resource Res* 40:W12504.
3. Schubert SD, Suarez MJ, Pegion PJ, Koster RD, Bacmeister JT (2004) *Science* 303:1855–1859.
4. Seager R, Kushnir Y, Herweijer C, Naik N, Velez J (2005) *J Clim* 18:4065–4088.
5. Sutton RT, Hodson DLR (2005) *Science* 309:115–118.
6. Dong B, Sutton RT, Scaife AA (2006) *Geophys Res Lett* 33:L08705, doi: 10.1029/2006GL025766.
7. Gershunov A, Barnett TP (1998) *Bull Am Meteorol Soc* 79:2715–2725.
8. Verdon DC, Franks SW (2006) *Geophys Res Lett* 33:L06712, doi: 10.1029/2005GL025052.
9. McCabe GJ, Dettinger MD (1999) *Int J Climatol* 19:1399–1410.
10. Westerling AL, Swetnam TW (2003) *EOS* 84:545–560.
11. Norman SP, Taylor AH (2003) *J Biogeogr* 30:1081–1092.
12. Taylor AH, Beaty RM (2005) *J Biogeogr* 32:425–438.
13. Schoennagel T, Veblen TT, Romme WH, Sibold JS, Cook ER (2005) *Ecol Appl* 15:2000–2014.
14. Collins BM, Omi PN, Chapman PL (2006) *Can J For Res* 36:699–709.
15. Sibold JS, Veblen TT (2006) *J Biogeog* 33:833–842.
16. Brown PM (2006) *Ecology* 87:2500–2510.
17. D'Arrigo RD, Cook ER, Wilson RJ, Allan R, Mann M E (2005) *Geophys Res Lett* 32:L03711, doi:10.1029/2004GL022055.
18. D'Arrigo R, Villalba R, Wiles G (2001) *Clim Dyn* 18:219–224.
19. Gray ST, Graumlich LJ, Betancourt JL, Pederson GD (2004) *Geophys Res Lett* 31:L12205, doi:10.1029/2004GL019932.
20. Brown PM, Wu R (2005) *Ecology* 86:3030–3038.
21. Swetnam TW, Betancourt JL (1990) *Science* 249:1017–1020.
22. Veblen TT, Kitzberger T, Donnegan J (2000) *Ecol Appl* 10:1178–1195.
23. Heyerdahl EK, Brubaker LB, Agee JK (2002) *Holocene* 12:597–604.
24. Hessl AE, McKenzie D, Schellhaas R (2004) *Ecol Appl* 14:425–442.
25. Kitzberger T, Swetnam TW, Veblen TT (2001) *Global Ecol Biogeogr* 10:315–326.
26. Grissino-Mayer HD, Swetnam TW (2000) *Holocene* 10:213–220.
27. Mann ME, Bradley RS, Hughes MK (1998) *Nature* 392:779–787.
28. Dettinger MD, Cayan DR, Diaz HF, Meko DM (1998) *J Clim* 11:3095–3111.
29. Gedalof Z, Peterson DL, Mantua NJ (2005) *Ecol Appl* 15:154–174.
3. Mantua NJ, Hare SR, Zhang Y, Wallace JM, Francis RC (1997) *Bull Am Meteor Soc* 78:1069–1080.
31. Enfield DB, Cid-Serrano L (2006) *Int J Climatol* 26:885–895.
32. Mann ME, Emanuel KA (2006) *EOS* 87:233, 238, 241.
33. Westerling AL, Hidalgo HG, Cayan DR, Swetnam TW (2006) *Science* 313:940–941.
34. Cook ER, Woodhouse CA, Eakin CM, Meko DM, Stahle DW (2004) *Science* 306:1015–1018.
35. Torrence C, Compo GP (1998) *Bull Am Meteor Soc* 79:61–78.